Effective versus standard Epstein loss figure in Fe-Si sheets.

Effective versus standard Epstein loss figure in Fe-Si sheets.

Enzo Ferrara[1], Carlo Appino[1], Luciano Rocchino[1], Carlo Ragusa[2],
Olivier de la Barrière[3], and Fausto Fiorillo[1]

[1] Istituto Nazionale di Ricerca Metrologica, Nanoscience and Materials Division, Torino, Italy
[2]Politecnico di Torino, Energy Department, Torino, Italy
[3]SATIE-ENS, UniverSud, Cachan, France

Abstract

The magnetic power losses have been measured at 50 Hz and different peak polarization values on different types of non-oriented and grain-oriented Fe-Si sheets using the Epstein frame, according to the current standards. The very same measurements have then been repeated by measuring polarization and tangential magnetic field by means of localized windings, centrally placed on the strips inside the Epstein frame windings, thereby retrieving the effective field and the true power loss figure. It is obtained that the ratio of the standard P_{epst} to the effective P_{eff} loss figure, which can be interpreted in terms of ratio of effective l_{eff} to conventional (l_m = 0.94 m) magnetic path length, evolves with the peak polarization J_p, showing, in general, a monotonic increase with increasing J_p. The deviation of P_{epst} from P_{eff} is observed to range from about -3 % in the non-oriented alloys at low inductions to about +5 % in the grain-oriented alloys at J_p = 1.8 T. This behavior finds a rationale in the existence of a polarization profile $J_p(x)$ measured along the strip length and in the dependence of P_{eff} on J_p, showing a power law $P_{eff}(J_p) \propto J_p^n$, with n >1 and increasing with J_p. The so calculated effective path length $l_{eff} = l_m \cdot P_{epst} / P_{eff}$ consistently show a monotonic increase with J_p, which is more relevant in the GO alloys.

Keywords: Magnetic power losses, Epstein frame, Magnetic steels.

1. Introduction

The 25 cm Epstein test-frame with a defined magnetic path length $l_m = 0.94$ m is a solidly assessed method for the characterization of the magnetic steel sheets. It ensures good measurement reproducibility and is widely adopted as an industry standard [1][2][3][4]. It is also well established that the specific features of the employed magnetic circuit, with the double overlapping corners and the ensuing inhomogeneous flux distribution, make the value of the measured quantities, namely the magnetic losses, different from the value of the true quantities [5][6]. True values could, however, be possibly accounted for by incorporating the complex response of the magnetic circuit into an effective magnetic path length l_{eff}, depending on the type of sheet, peak induction value, frequency, and type of excitation [7]. Should the effective (true) power loss figure P_{eff} be measured, one could express it in terms of standard power loss value P_{epst} according to

$$P_{\text{eff}} = P_{\text{epst}} \cdot l_{\text{m}} / l_{\text{eff}} . \quad (1)$$

Measurements of P_{eff} using a single strip tester and an H-coil were reported for non-oriented (NO) and grain-oriented (GO) sheets by Ahlers, et al. [8]. They found at 50 Hz $P_{epst} < P_{eff}$, that is $l_{eff} > l_m$ in all materials, with maximum difference of the order of 8% in GO sheets at $J_p = 1.7$ T. These authors justified their results in terms of effective length, expressed as $l_{eff} = l_0 + (\mu_l/2\mu_c)\cdot l_c$, the sum of the legs length l_0 and part of the corners length l_c, depending on the ratio of the leg to corner permeabilities μ_l and μ_c. A number of literature experiments [5] actually show scattered outcomes, both in NO and GO materials, with P_{epst} either higher or lower than P_{eff} and P_{epst} / P_{eff} generally decreasing with the peak polarization J_p. Marketos, et al. [7][9] have determined l_{eff} by measuring GO and NO sheets with conventional 25 cm and reduced 17.5 cm Epstein frames. They find, assuming identical flux distribution in the corners of the two frames, that l_{eff} is always higher than l_m (that is, $P_{epst} / P_{eff} > 1$) in GO high-permeability sheets and, in contrast with the results reported in [5], increasing with J_p.

In this paper we discuss measurements of power losses performed at 50 Hz on different types of NO and GO steel sheets, both according to the measuring standard (25 cm Epstein frame with $l_m = 0.94$ m) and by detecting the tangential field and the induction derivative by collinear narrow H- and B-coils windings, placed directly upon the steel strips at the centre of the Epstein legs. In this way, the true power loss $P_{eff}(J_p)$ is obtained in comparison with the standard loss figure $P_{epst}(J_p)$. A ratio P_{epst} / P_{eff} monotonically increasing with J_p is thus found in all materials. This can equivalently be expressed in terms of an effective path length similarly increasing with J_p.

2. Experimental method

The magnetic measurements were performed at 50 Hz under sinusoidal induction waveform on the NO and GO alloys listed in Table 1. Both conventional (CGO) and high-permeability (HGO) grain-oriented sheets were investigated. A calibrated hysteresisgraph-wattmeter with digital control of the induction waveform was used, where signal acquisition and A/D conversion is made by means of a 12-bit 500 MHz HDO4054 LeCroy oscilloscope. The whole measuring process is performed within an Agilent VEE environment. The NO and GO alloys were tested in the polarization intervals 0.5 T – 1.5 T and 1.0 T – 1.8 T, respectively, with either eight or twelve strips inserted in the Epstein frame, depending on the sheet thickness. For any given material, a standard measurement was first made, followed by measurements with the centrally placed local windings. The arrangement of the 17 mm wide *H*- and *B*-coils, which are stuck together and placed inside the Epstein windings, is schematically shown in Fig. 1. The *H*-coil (turn-area $N_H S_H = 2.11 \cdot 10^{-2}$ m^2, thickness ~ 1.5 mm) is made of a few hundred turns (wire diameter 0.05 mm) wound on a rigid fibreglass plate and calibrated inside a field reference setup [10]. The 50-turn *B*-coil enwraps the *H*-coil and the strips under test. The air-flux contribution is usually negligible, but it is in any case compensated via software. Once the single standard Epstein measurement of the power loss $P_{epst}(J_{0p})$ at a given polarization J_{0p} is done, the local dB/dt and dH_{eff}/dt signals are simultaneously detected, under the identical exciting conditions, at a significant number of points, from corner to corner, along the length of the Epstein leg, amplified by calibrated low-noise amplifiers SR560, and integrated, These local measurements are then identically repeated on the other legs and the results are averaged. They provide the behaviours of $J(x)$ and $H_{eff}(x)$ as a function of the distance x from the centre of the leg for the Epstein measured polarization J_{0p}. The distance x ranges between -110 mm and +110 mm. Finally, the *H*- and *B*-coils are moved to the centre of the leg (x = 0) and the measurement of $P_{eff}(J_{0p})$ is performed by imposing the local dJ/dt sinusoidal with peak polarization value $J_p(0) = J_{0p}$. It is remarked that across the 17 mm wide region occupied by the coils centred at $x = 0$ the polarization is highly uniform. Given the low field levels involved, a certain background noise in the dH_{eff}/dt signal is inevitable. This is dealt with by repeating the very same measurement a number of times, to make the random uncertainty contribution negligible. The process is further repeated on the other legs and the results are averaged.

3. Experimental results and discussion

The general outcome of the measurements performed on the six different types of soft magnetic steels described in Table 1, two NO sheets of thickness 0.194 mm and 0.343 mm, two conventional and two high-permeability GO sheets, of thickness ranging between 0.255 and 0.295 mm, is that the standard Epstein loss figure P_{epst} can either overestimate or underestimate the effective power loss P_{eff}, but the ratio P_{epst} / P_{eff} is always a monotonically increasing function of J_p. The local $J_p = J_p(0)$ value involved in the measurement of P_{eff} is obviously made to coincide with the polarization value J_{0p} previously determined through the whole Epstein secondary winding. While this result may appear partly ad odd with previous literature outcomes [5][8], we shall observe in the following how the behavior of P_{epst} / P_{eff} can be justified in terms of inhomogeneity of the induction along the Epstein legs and the power law dependence of P_{eff} on J_p. Let us therefore observe in Fig. 2 the overall experimental behaviors of $(P_{epst} - P_{eff})/ P_{eff}$ versus J_p and of the related effective magnetic path length $l_{eff} = l_m \cdot (P_{epst}/P_{eff})$. Similar trends versus J_p are followed by the NO and GO materials, but the standard power loss P_{epst} becomes significantly higher, around 4 % – 5 %, than the true loss P_{eff} at the highest J_p values in the GO sheets. Table 2 provides a comparison of the measured power losses P_{epst} and P_{eff}.

In order to find a rationale for the J_p dependent relationship between P_{epst} and P_{eff}, it is useful to analyze the distribution of field and polarization along the magnetic circuit, as retrieved by the previously described local measurements. To start with, we provide an example in Fig. 3, concerning the NO-2 sheet, of field decomposition along a leg of the frame for a standard Epstein measurement at a given polarization value J_p. The solenoid surrounding each leg has length $2L$ = 195 mm. By subtracting the effective field $H_{eff}(x)$, measured by sliding the H-coil along the leg, from the field $H_{sol}(x)$ applied by the primary solenoid, we obtain the behavior of the magnetostatic field $H_d(x)$. This exerts a demagnetizing action towards the strip portion of length $2L$ underlying the Epstein winding, adding instead to H_{sol} towards the corners, to eventually impose a magnetic path length l_{eff} longer than the solenoid length. The effect of H_d is less important at high inductions, where the permeability is lower and the free poles are more localized around the solenoid edges. The distribution of the polarization $J_p(x)$ along $2L$ is however moderately affected, as shown by the examples regarding the samples NO-2 and HGO-1 shown in Fig. 4. These curves are representative of the flux distribution found in all materials and bring to light the fact that, because of the strong non-linear dependence of the power loss on J_p, the true loss value cannot be recovered by a standard Epstein measurement, adjusted through a simple constant (in this case the conventional magnetic path length l_m). By denoting the polarization measured through the secondary Epstein winding $J_0(t) = J_{0p}\sin(\omega t)$, where $J_{0p} = \frac{1}{2L}\int_{-L}^{L} J_p(x)\,dx$, we can write the power loss per unit volume measured with the standard method

$$P_{epst}(J_{0p}) = \frac{1}{T}\int_0^T H_{epst}(t)\cdot J_{0p}\omega\cos(\omega t)dt \quad , \tag{2}$$

where $H_{epst}(t) = N_H\, i_H(t)\, /\, l_m$, N_H is the number of turns of the primary winding and $i_H(t)$ is the magnetizing current. The true power loss corresponding to the condition met with the standard Epstein measurement is therefore given by the average of the local $P_{eff}(x)$ across the length $2L$

$$P_{eff}(J_{0p}) = \frac{1}{2L}\int_{-L}^{L} dx\ \frac{1}{T}\int_0^T H_{eff}(t,x)\cdot J_p(x)\cdot\omega\cos(\omega t)dt = \frac{1}{2L}\int_{-L}^{L} P_{eff}(J_p(x))\,dx . \tag{3}$$

We thus obtain the effective magnetic path length corresponding to such condition

$$l_{eff}(J_{0p}) = l_m\cdot\frac{P_{epst}(J_{0p})}{P_{eff}(J_{0p})} . \tag{4}$$

The quantity $P_{eff}(J_{0p})$ can be measured, according to Eq. (3), by integrating the previously discussed local measurements, which are represented as a function of J_p in Fig. 5, over the $J_p(x)$ distribution shown in Fig. 4. This is easily done through knowledge of the measured dependence of $P_{eff}(J_p)$ on J_p, which, as shown in Fig. 5, follows a power law $P_{eff}(J_p) \propto J_p^{\,n}$, with n an increasing function of J_p. By introducing the $P_{eff}(J_{0p})$ calculated by Eq. (3), we obtain the behavior of $l_{eff}(J_{0p})$ in the different materials shown in Fig. 6. On the other hand, the previously defined $P_{eff}(J_p)$ (Fig. 2) is the true loss measured at $x = 0$ when $J_p(0) = J_p$, which is compared with the Epstein power loss when the secondary winding provides the same polarization value J_p. $l_{eff}(J_p)$ is correspondingly defined through Eq. (1). Consequently, $l_{eff}(J_{0p})$ and $l_{eff}(J_p)$ do not usually coincide. $l_{eff}(J_{0p})$ is, in any case, the magnetic path length to be applied in substitution of l_m when making the standard Epstein testing at 50 Hz at the specific measured polarization level J_{0p}. It takes into account the fact that the peak polarization J_{0p} measured by the secondary Epstein winding is the average of $J_p(x)$ between ± L, according to the behaviors of $J_p(x)$ shown in Fig. 4. It will coincide with $l_{eff}(J_p)$ for homogeneous $J_p(x)$ across the solenoid length $2L$, a limiting unattainable condition. The calculated $l_{eff}(J_{0p})$ and the measured $l_{eff}(J_p)$ nevertheless display quite similar increasing trends vs. J_p, both in NO and GO alloys, as illustrated by their behaviors shown in Fig. 6. It is appreciated the fact that, as shown in Figs. 2 and 6, the effective magnetic path length in the GO alloys tends to be higher than in the NO sheets, besides being larger than the conventional Epstein value l_m = 0.94 m. This implies that P_{epst} / P_{eff} is similarly higher. The present results actually show that $J_p(x)$ is more homogeneous in the GO strips (see the example shown in Fig. 4), thereby better approaching the ideal condition of perfectly homogeneous magnetization over the whole 1m long Epstein circuit.

4. Conclusions

Measurements of the true power losses in different types of non-oriented and grain-oriented materials using localized *H*- and *B*-coils placed inside the legs of a standard 25 cm Epstein frame have been compared, upon a range of peak polarization values, with the loss figures obtained according to the usual procedure prescribed by the measuring standards. It is found that true P_{eff} and standard P_{epst} power loss figures are in a relationship dependent on the imposed peak polarization value J_p , with the ratio P_{epst} / P_{eff} exhibiting a monotonical increase with J_p in all materials in the investigated polarization range 0.5 T ≤ J_p ≤ 1.8 T. This behavior, which can be interpreted in terms of an effective magnetic path length l_{eff}, to be used as a substitute for the conventional fixed length l_m = 0.94 m in the expression for the applied field, is justified in terms of non-uniform profile of the polarization $J_p(x)$ along the strip portion underlying the Epstein secondary winding and non-linear increase of P_{eff} with J_p. The effective path length $l_{eff}(J_p)$ can then be calculated, by which true and Epstein power losses are reconciled.

References

[1] J. Sievert, H. Ahlers, F. Fiorillo, L. Rocchino, M. Hall and L. Henderson, Magnetic measurements on electrical steels using Epstein and SST method, *PTB-Bericht* **E-74**(2001), 1–28.

[2] C. Appino, E. Ferrara, F. Fiorillo, L. Rocchino, C. Ragusa, J. Sievert, T. Belgrand, C. Wang, P. Denke, S. Siebert, Y. Norgren, K. Gramm, S. Norman, R. Lyke, M. Albrecht, X. Zhou, W. Fan, X. Guo, M. Hall, "International comparison on SST and Epstein measurements in grain-oriented Fe-Si sheet steel", *Int. J. Appl. Electromagnetics Mech.* **48** (2015), 123-133, doi: 10.3233/JAE-151978.

[3] IEC Standard Publication 60404-2, Methods of measurement of the magnetic properties of electrical steel sheet and strip by means of the Epstein frame, (Geneva: IEC Central Office, 1996).

[4] ASTM Publication A343.97, Standard test method for alternating-current magnetic properties of amorphous materials at power frequencies using wattmeter-ammeter-voltmeter method using wattmeter-ammeter-voltmeter method and 25-cm Epstein test frame" (West Conshohocken, PA: ASTM International, 1993).

[5] J.D. Sievert, Determination of the AC magnetic power loss of electrical steel sheet: present status and trends, *IEEE Trans. Magn.* **20** (1984), 1702-1706, doi: 10.1109/TMAG.1984.1063278.

[6] E. Antonelli, E. Cardelli, A. Faba, Epstein frame: how and when it can be really representative about the magnetic behavior of laminated magnetic steels, *IEEE Trans. Magn.* **41** (2005), 1516-1519, doi: 10.1109/TMAG.2005.845072.

[7] P. Marketos, S. Zurek, and A.J. Moses, A method for defining the mean path length of the Epstein frame, *IEEE Trans. Magn.* **43** (2007), 2755-2757, doi: 10.1109/TMAG.2007.894124.

[8] H. Ahlers, J.D. Sievert, and Qu.-ch. Qu, Comparison of a single strip tester and Epstein frame measurements, *J. Magn. Magn. Mater.* **26** (1982), 176-178, doi:10.1016/0304-8853(82)90145-7.

[9] P. Marketos, S. Zurek, and A.J. Moses, Calculation of the mean path length of the Epstein frame under non-sinusoidal excitations using the double Epstein method, *J. Magn. Magn. Mater.,* **320** (2008), 2542-2545, doi: 10.1016/j.jmmm.2008.04.085.

[10] F. Fiorillo, G.F. Durin, and L. Rocchino: "A reference system for the measurement of low-strength magnetic flux density", *J. Magn. Magn. Mater*, **304** (2006), e540-e542.

Table 1

Physical parameters of the investigated non-oriented (NO), conventional (CGO) and high-permebility (HGO) grain-oriented steel sheets.

Fe-Si alloy	Composition	Thickness (mm)	Density (kg/m^3)	Resistivity (□□m)
NO-1	Fe-(**3.2** wt%)Si	0.194	7650	$52 \cdot 10^{-8}$
NO-2	Fe-(**3.5** wt%)Si	0.343	7600	$56.4 \cdot 10^{-8}$
CGO-1	Fe-(**3** wt%)Si	0.255	7650	$48 \cdot 10^{-8}$
CGO-2		0.261		
HGO-1		0.257		
HGO-2		0.295		

Table 2

Power loss at 50 Hz obtained by the standard Epstein measurement (P_{epst}) and the localized measurement (P_{eff}) as a function of peak polarization on three different Fe-Si sheets.

f = 50 Hz	NO-1		CGO-2		HGO-1	
J_p (T)	P_{epst} (W/kg)	P_{eff} (W/kg)	P_{epst} (W/kg)	P_{eff} (W/kg)	P_{epst} (W/kg)	P_{eff} (W/kg)
0.50	0.241	0.248	--	--	--	--
0.75	0.480	0.489	--	--	--	--
1.0	0.784	0.755	0.345	0.343	0.303	0.299
1.2	1.125	1.135	0.499	0.498	0.431	0.426
1.4	1.656	1.665	--	--	--	--
1.5	2.07	2.050	0.811	0.787	0.681	0.664
1.7	--	--	1.198	1.154	0.914	0.874
1.8	--	--	1.587	1.514	1.123	1.063

Figure captions

Fig. 1 – Arrangement of the local sensing coils inside a leg of the Epstein frame. The flat multiturn *H*-coil (thickness ~ 1.5 mm) is placed in contact with the Epstein strip surface and the *B*-coil is wound around it and the steel strips. The coils are about 17 mm wide and can slide along the whole length of the Epstein leg.

Fig. 2 – The experimental dependence on J_p of the ratio of standard to true power losses P_{epst}/P_{eff} in NO and in conventional (CGO) and high-permeability (HGO) Fe-Si alloys (a) is paralleled by the behavior of the effective magnetic path length l_{eff} (b).

Fig. 3 – Effective field H_{eff} measured versus the distance x from the Epstein leg centre in the NO-2 sheet. It is $H_{eff} = H_{sol} - H_d$, the difference between the field H_{sol} generated by the primary winding and the field H_d originating from the free poles distributed along the strip length. To note the demagnetizing and magnetizing effect of H_d beneath and outside the solenoid length. The horizontal dotted line shows the conventional field H_{epst}, calculated assuming the magnetic path length $l_m = 0.94$ m.

Fig. 4 – Examples of measured distribution of the reduced polarization $J(x)$ / $J(0)$ upon the portion of strip length underlying the Epstein secondary winding in the NO-2 and HGO-1 sheets.

Fig. 5 – The measured effective power loss $P_{eff}(J_p)$ increases with the peak polarization J_p according to a power law $P_{eff} \propto J_p^n$, with n an increasing function of J_p.

Fig. 6 – Effective magnetic path lengths $l_{eff}(J_{0p})$ and $l_{eff}(J_p)$ versus peak polarization in the investigated NO and GO steel sheets. $l_{eff}(J_{0p})$ is calculated through Eqs. (2)–(4). It permits one to retrieve the true power loss value from the standard loss figure for peak polarization J_{0p} measured with the secondary Epstein winding. $l_{eff}(J_p)$ is the same quantity obtained for $J_p = J_p(0)$, where $J_p(0)$ is the polarization measured at the centre of the Epstein leg.

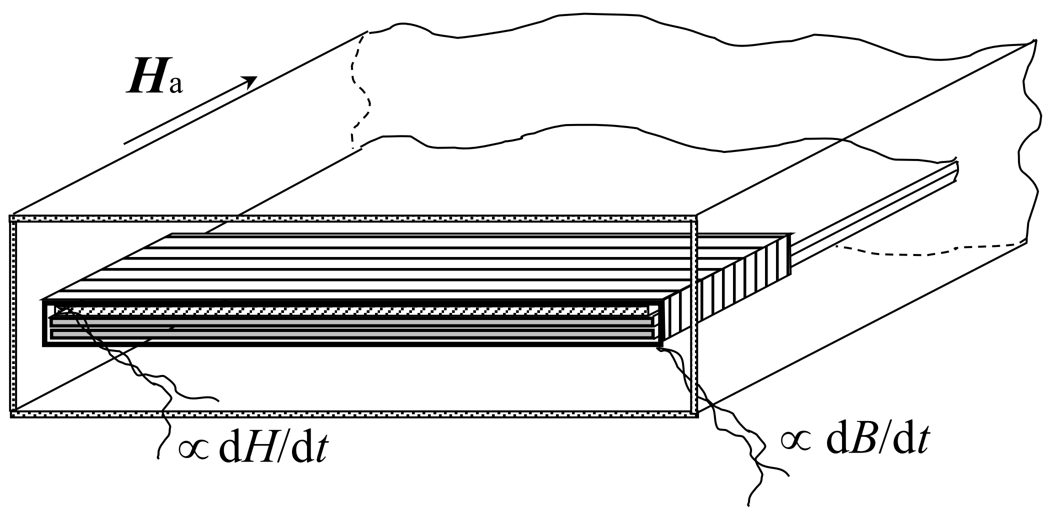

Fig. 1 – Arrangement of the local sensing coils inside a leg of the Epstein frame. The flat multiturn H-coil (thickness ~ 1.5 mm) is placed in contact with the Epstein strip surface and the B-coil is wound around it and the steel strips. The coils are about 17 mm wide and can slide along the whole length of the Epstein leg.

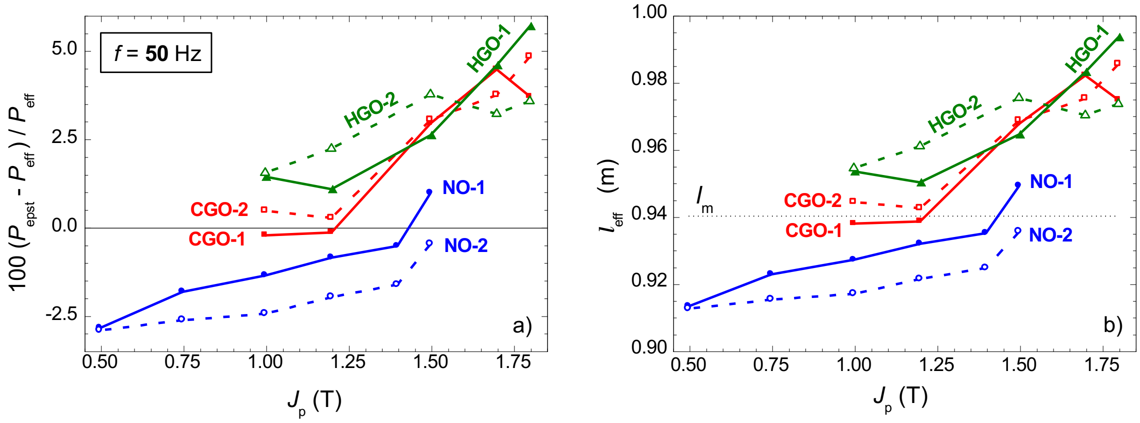

Fig. 2 – The experimental dependence on J_p of the ratio of standard to true power losses P_{epst}/P_{eff} in NO and in conventional (CGO) and high-permeability (HGO) Fe-Si alloys (a) is paralleled by the behavior of the effective magnetic path length l_{eff} (b).

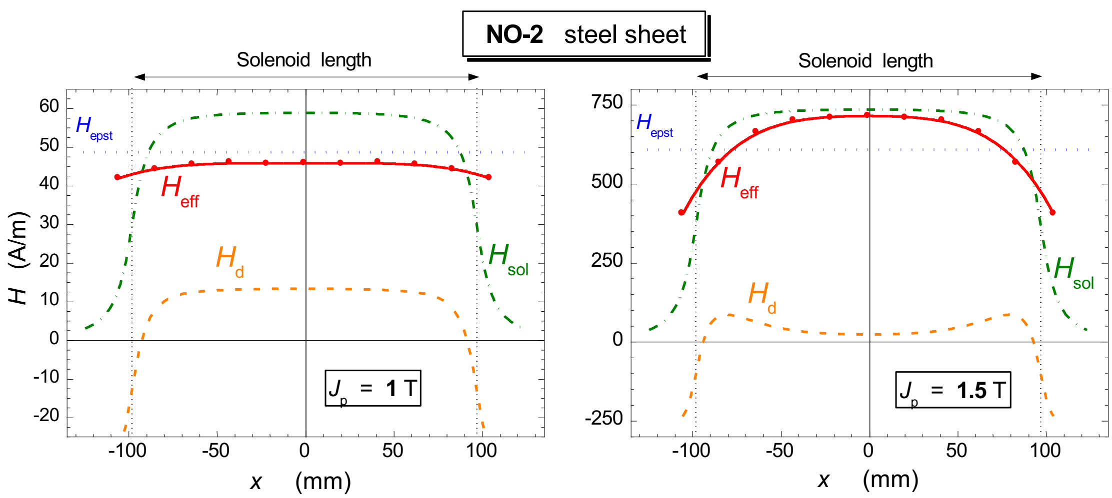

leg

H_{sol}

les

ing

ine

gth

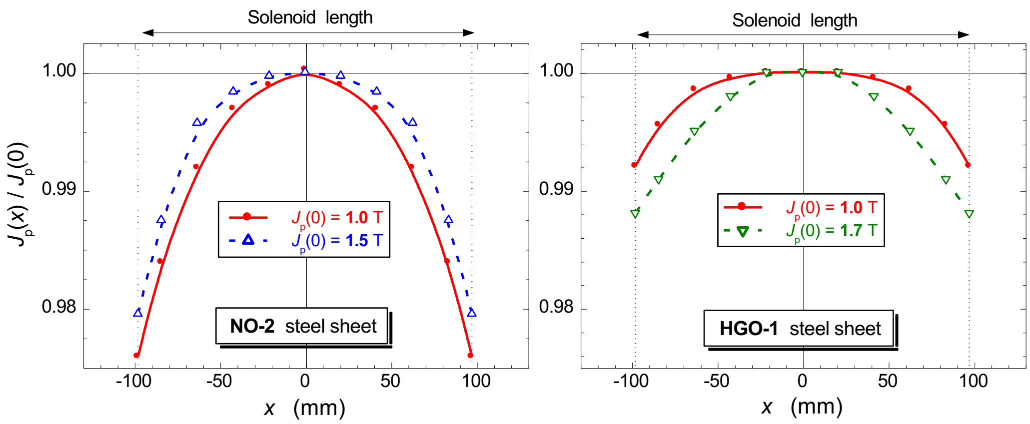

Fig. 4 – Examples of measured distribution of the reduced polarization $J(x)$ / $J(0)$ upon the portion of strip length underlying the Epstein secondary winding in the NO-2 and HGO-1 sheets.

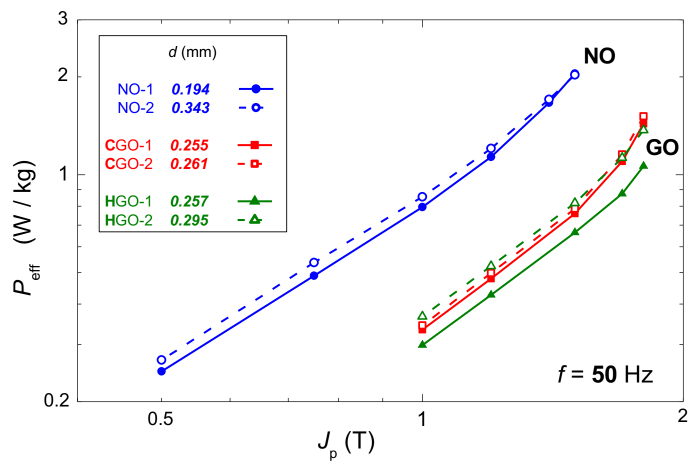

Fig. 5 – The measured effective power loss $P_{eff}(J_p)$ increases with the peak polarization J_p according to a power law $P_{eff} \propto J_p^n$, with n an increasing function of J_p.

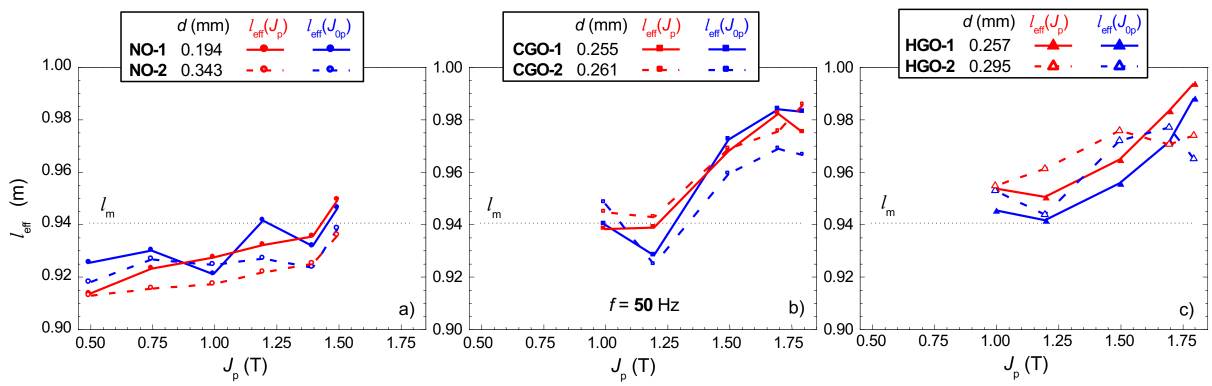

Fig. 6 – Effective magnetic path lengths $l_{eff}(J_{0p})$ and $l_{eff}(J_p)$ versus peak polarization in the investigated NO and GO steel sheets. $l_{eff}(J_{0p})$ is calculated through Eqs. (2)–(4). It permits one to retrieve the true power loss value from the standard loss figure for peak polarization J_{0p} measured with the secondary Epstein winding. $l_{eff}(J_p)$ is the same quantity obtained for $J_p = J_p(0)$, where $J_p(0)$ is the polarization measured at the centre of the Epstein leg.